Article

Cell Reports

miR-137 Modulates a Tumor Suppressor Network-Inducing Senescence in Pancreatic Cancer Cells

Graphical Abstract

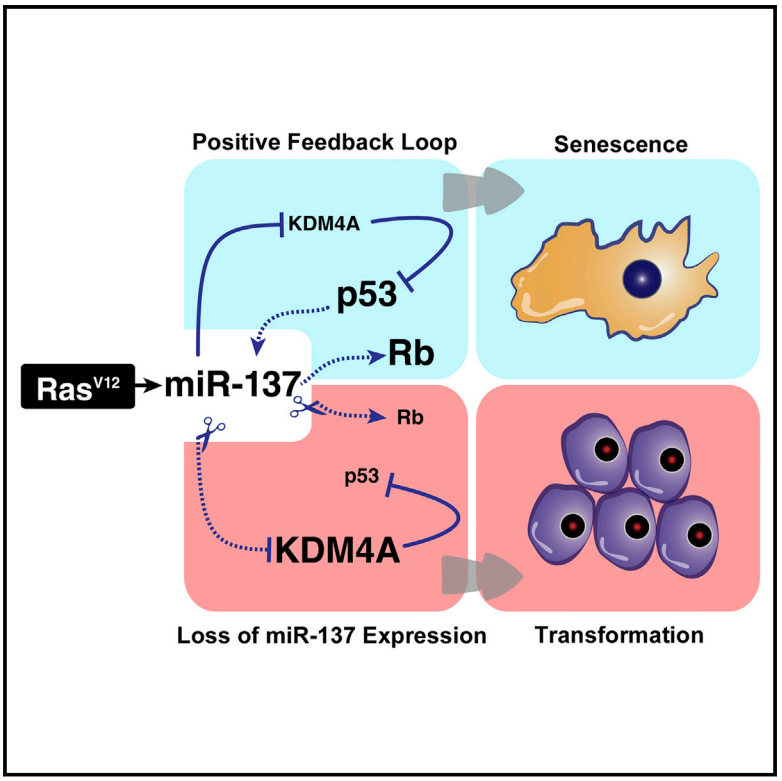

Authors

Mathieu Neault, Frédérick A. Mallette, Stéphane Richard

Correspondence

fa.mallette@umontreal.ca (F.A.M.), stephane.richard@mcgill.ca (S.R.)

In Brief

Depletion of KDM4A in response to Ras is a key event mediating Ras-induced senescence in normal cells. Neault et al. show that Ras-induced miR-137 targets KDM4A and activates downstream p53 and p16^{INK4A} tumor suppressor pathways to promote cell-cycle arrest and senescence.

Highlights

- miR-137 triggers the p53 and p16^{INK4A} tumor suppressor pathways
- KDM4A is a target of miR-137 during Ras-induced senescence
- Loss of miR-137 contributes to the bypass of Ras-induced senescence
- Restoration of miR-137 expression induces senescence in pancreatic cancer cells

Neault et al., 2016, Cell Reports *14*, 1966–1978
March 1, 2016
http://dx.doi.org/10.1016/j.celrep.2016.01.068

CellPress

OPEN ACCESS
CellPress

Cell Reports
Article

miR-137 Modulates a Tumor Suppressor Network-Inducing Senescence in Pancreatic Cancer Cells

Mathieu Neault,[1,2] Frédérick A. Mallette,[3,4,*] and Stéphane Richard[1,2,*]
[1]Terry Fox Molecular Oncology Group and the Bloomfield Center for Research on Aging, Segal Cancer Centre, Lady Davis Institute for Medical Research, Sir Mortimer B. Davis Jewish General Hospital, Montréal, QC H3T 1E2, Canada
[2]Departments of Oncology and Medicine, McGill University, Montréal, QC H3T 1E2, Canada
[3]Chromatin Structure and Cellular Senescence Research Unit, Maisonneuve-Rosemont Hospital Research Centre, Montréal, QC H1T 2M4, Canada
[4]Department of Medicine, Université de Montréal, C.P. 6128, Succ. Centre-Ville, Montréal, QC H3C 3J7, Canada
*Correspondence: fa.mallette@umontreal.ca (F.A.M.), stephane.richard@mcgill.ca (S.R.)
http://dx.doi.org/10.1016/j.celrep.2016.01.068

SUMMARY

Activating *K-Ras* mutations occurs frequently in pancreatic cancers and is implicated in their development. Cancer-initiating events, such as oncogenic *Ras* activation, lead to the induction of cellular senescence, a tumor suppressor response. During senescence, the decreased levels of KDM4A lysine demethylase contribute to p53 activation, however, the mechanism by which KDM4A is downregulated is unknown. We show that miR-137 targets *KDM4A* mRNA during Ras-induced senescence and activates both p53 and retinoblastoma (pRb) tumor suppressor pathways. Restoring the KDM4A expression contributed to bypass of miR-137-induced senescence and inhibition of endogenous miR-137 with an miRNA sponge-compromised Ras-induced senescence. miR-137 levels are significantly reduced in human pancreatic tumors, consistent with previous studies revealing a defective senescence response in this cancer type. Restoration of miR-137 expression inhibited proliferation and promoted senescence of pancreatic cancer cells. These results suggest that modulating levels of miR-137 may be important for triggering tumor suppressor networks in pancreatic cancer.

INTRODUCTION

Escape from oncogene-induced senescence (OIS) potentiates malignant transformation. In human fibroblasts, defects in the ARF/p53 and $p16^{INK4A}$/pRb tumor suppressor pathways are required to bypass OIS (Lowe et al., 2004). Not surprisingly, therefore, these pathways are frequently altered in *Ras*-driven cancers, since hyperactivation of Ras triggers p53- and pRb-dependent OIS and growth inhibition in normal cells (Serrano et al., 1997). OIS represents a critical tumor-suppressive mechanism in vivo (Braig et al., 2005; Chen et al., 2005; Collado et al., 2005; Kuilman et al., 2010; Michaloglou et al., 2005). In untransformed cells, sustained MAP kinase signaling induced by activated Ras leads to senescence, i.e., permanent G_1 arrest (Lin et al., 1998; Serrano et al., 1997; Zhu et al., 1998). During oncogenic stress, p53 stimulates many genes that promote cellular senescence, including those encoding the CDK inhibitor $p21^{cip/waf1}$ (hereafter p21) (Lowe et al., 2004), the promyelocytic leukemia (PML) protein (Pearson et al., 2000), and plasminogen activator inhibitor type 1 (PAI-1, Kunz et al., 1995). p21 mediates G_1/S arrest by inhibiting G_1 cyclin-dependent kinases (McConnell et al., 1998). PML recruits p53 to nuclear bodies to stimulate transcription of p53 targets, including p53 itself (de Stanchina et al., 2004; Ferbeyre et al., 2000). The product of the alternative reading frame of the *INK4A/ARF* locus, $p19^{ARF}$, also is induced by oncogenes (Lowe and Sherr, 2003). $p19^{ARF}$ sequesters MDM2 to the nucleolus, which in turn protects p53 from MDM2-associated proteasomal degradation (Weber et al., 1999). Expression of oncogenes also leads to upregulation of the CDK inhibitor $p16^{INK4A}$ (Gan et al., 2008; Lin et al., 1998), in turn blocking inhibitory phosphorylation of pRb (Ruas and Peters, 1998) and of consequent (Chellappan et al., 1991; Nevins et al., 1991) E2F-dependent transcription of genes required for G_1/S progression (Chicas et al., 2010).

The *K-Ras* member of the *Ras* GTPase family is mutated in >95% of pancreatic ductal adenocarcinoma (PDAC) (Stephen et al., 2014), and the *INK4A/ARF* and *TP53* loci are mutated in ~80% of such cases. Moreover, such mutations are associated with the more malignant and aggressive forms of PDAC (Moir et al., 2014). Re-establishment of p53 in *K-Ras*-driven tumors leads to tumor regression in vivo (Dickins et al., 2005), while restoration of $p16^{INK4A}$ in *K-Ras*-driven pancreatic cancer cells inhibits clonogenic proliferation (Rabien et al., 2012), further indicating the crucial roles of p53 and $p16^{INK4A}$ in pancreatic tumor suppression.

The precise molecular basis for activation of the ARF/p53 and $p16^{INK4A}$/pRb pathways during OIS remains unclear. We recently reported the reduction of KDM4A lysine demethylase (also

known as JMJD2A) levels upon Ras activation, which in turn stimulates expression of the *CHD5* tumor suppressor; furthermore, overexpression of KDM4A in $p16^{INK4A}$-depleted fibroblasts led to bypass of OIS (Mallette and Richard, 2012). In addition KDM4A cooperated with Ras in the transformation of primary cells by inhibiting the p53 pathway, suggesting that KDM4A depletion following oncogenic signaling modulates p53 activation.

KDM4A catalyzes the removal of di- and tri-methylated lysines 9 and 36 of histone H3 (H3K9/H3K36) via a dioxygenase reaction mechanism (Tsukada et al., 2006; Whetstine et al., 2006). KDM4A possesses a JmjC catalytic domain and its catalytic activity is dependent on Fe^{2+} and α-ketoglutarate (Tsukada et al., 2006). This demethylase participates in multiple processes, including the DNA damage response (Mallette et al., 2012), gene amplification (Black et al., 2013), the immune response (Jin et al., 2014), and the transcriptional activation of p53 (Mallette and Richard, 2012). Chromatin immunoprecipitation (ChIP) experiments revealed binding of KDM4A to promoter regions of *ASCL2* (Zhang et al., 2005), *CHD5*, *PANX2*, and *PPIC* (Mallette and Richard, 2012). In KDM4A-depleted cells, the p53 response is activated as assessed by the nuclear translocation of p53 and the increased expression of p53 targets, such as p21 and PML (Mallette and Richard, 2012). Initially identified as a tumor suppressor gene in neuroblastoma (Thompson et al., 2003), *CHD5* was later found to block tumorigenesis in vivo by positively regulating the *INK4A/ARF* locus (Mallette and Richard, 2012). Furthermore, loss of *CHD5* was shown to inhibit OIS (Bagchi et al., 2007). Following transcriptional repression of *CHD5*, KDM4A can counteract CHD5-dependent activation of the p53 pathway during Ras-induced senescence (Mallette and Richard, 2012). Decreased KDM4A expression following oncogenic stimulation seems to be a crucial determinant of OIS, but the mechanism responsible for KDM4A downregulation remains elusive.

Several studies have revealed emerging roles for microRNAs (miRNAs) in the regulation of cellular senescence. miR-372 and miR-373 were characterized as oncogenic miRNAs collaborating with *Ras* through suppression of *LATS2*, an intermediate of p53-mediated CDK inhibition (Voorhoeve et al., 2006). Furthermore, the *miR-17-92* gene cluster promotes malignant transformation, and miR-37/20a encoded within this cluster can bypass OIS (Hong et al., 2010). Conversely, increased *Ras* expression was correlated with *Let-7* depletion in lung cancer (Johnson et al., 2005), suggesting that miRNAs also can exert tumor-suppressive functions. In addition, p53 was shown to activate transcription, and maturation, of several miRNAs involved in cell-cycle arrest and senescence (Feng et al., 2011).

Herein we show that miR-137 targets KDM4A during Ras-induced senescence, leading to activation of the p53/pRb tumor suppressor pathways. Ectopic expression of miR-137 was sufficient to stimulate senescence in a p53- and pRb-dependent manner. Inactivation of miR-137 compromised Ras-induced senescence and decreased p21 mRNA levels. Finally, miR-137 levels were significantly reduced in human pancreatic tumors, and its re-expression induced cellular senescence in PANC1 cells. These findings suggest that the modulation of miR-137/KDM4A regulation may have therapeutic value in pancreatic cancer.

RESULTS

Identification of miR-137 as a Regulator of KDM4A

KDM4A protein levels are decreased during Ras-induced senescence, thereby relieving the *CHD5* promoter from negative regulation and allowing increased p53 expression (Mallette and Richard, 2012). In addition, *KDM4A* mRNA is significantly reduced during OIS, while the levels of *KDM4B* and *KDM4C* paralogs remain unchanged (Figure 1A), suggesting that diminished KDM4A activity may contribute to OIS. Indeed, *KDM4A* depletion using small interfering RNAs (siRNAs) induced premature senescence (Figures S1A and S1B) associated with an increase in *CHD5* mRNA levels (Figure S1C), consistent with previous findings (Mallette and Richard, 2012). However, the molecular mechanism responsible for the downregulation of *KDM4A* during OIS remains to be elucidated. We hypothesized that modulation of miRNA activity might be responsible for downregulation of *KDM4A* during OIS. Using miRANDA (http://www.microrna.org/microrna/home.do) and TARGETSCAN (http://www.targetscan.org/) algorithms (Enright et al., 2003; Lewis et al., 2003), we identified miR-137, miR-145, and miR-220c as predicted to target the 3′ UTR of *KDM4A* (Figures 1B and 1C). Interestingly, miR-137 and miR-145 are downregulated in various cancer types, suggesting that they may function as tumor suppressors (Bemis et al., 2008; Iorio et al., 2005; Kozaki et al., 2008; Nilsson et al., 2015; Silber et al., 2008).

To examine whether miR-137, miR-145, and/or miR-220c regulate KDM4A levels during OIS, we first measured levels of these miRs using qRT-PCR in senescent IMR90 normal diploid lung fibroblasts expressing $H\text{-}Ras^{V12}$. Mature miR-137 levels significantly increased, while miR-145 decreased and miR-220c levels did not change in $H\text{-}Ras^{V12}$-expressing cells (Figure 1D). We also documented a substantial increase (~2-fold) in miR-137 levels as early as 1 day after Ras induction, concomitant with a decrease of *KDM4A* mRNA levels (>2-fold; Figure S2A). *KDM4A* mRNA seemed to be stabilized at day 1 post-$H\text{-}Ras^{V12}$ induction, while miR-137 expression progressively increased >5-fold after 5 days (Figure S2A).

Since miR-137 was the only *KDM4A*-targeting candidate miRNA whose expression increased during OIS, we focused on the role of this miRNA. To evaluate its potential effect on *KDM4A*, we overexpressed mature miR-137 levels in IMR90 fibroblasts using miRNA mimics. The relative levels of *KDM4A* mRNA and a previously described miR-137 target, *CDC42* (Liu et al., 2011), were significantly reduced relative to miR-67 (Figure 1E), a *Caenorhabditis elegans*-specific miRNA (Sharma et al., 2009). The mRNA level of *CHD5*, a transcriptional target of *KDM4A* (Mallette and Richard, 2012), was increased following transfection with miR-137, consistent with decreased KDM4A mRNA expression and protein levels (Figure 1E).

The reduced level of KDM4A protein was confirmed subsequently by immunoblotting in U2OS and IMR90 fibroblasts (Figure 1F), and p53 protein was increased upon miR-137 treatment (Figure 1F), consistent with the increase in the p53-positive regulator *CHD5* (Mallette and Richard, 2012; Thompson et al., 2003). The *KDM4A* 3′ UTR harbors two miR-137 seed sequences that we termed miR-137 response elements (MREs) 1 and 2 (Figures 1B and 1C; MRE1 and MRE2). *Renilla* luciferase reporter genes

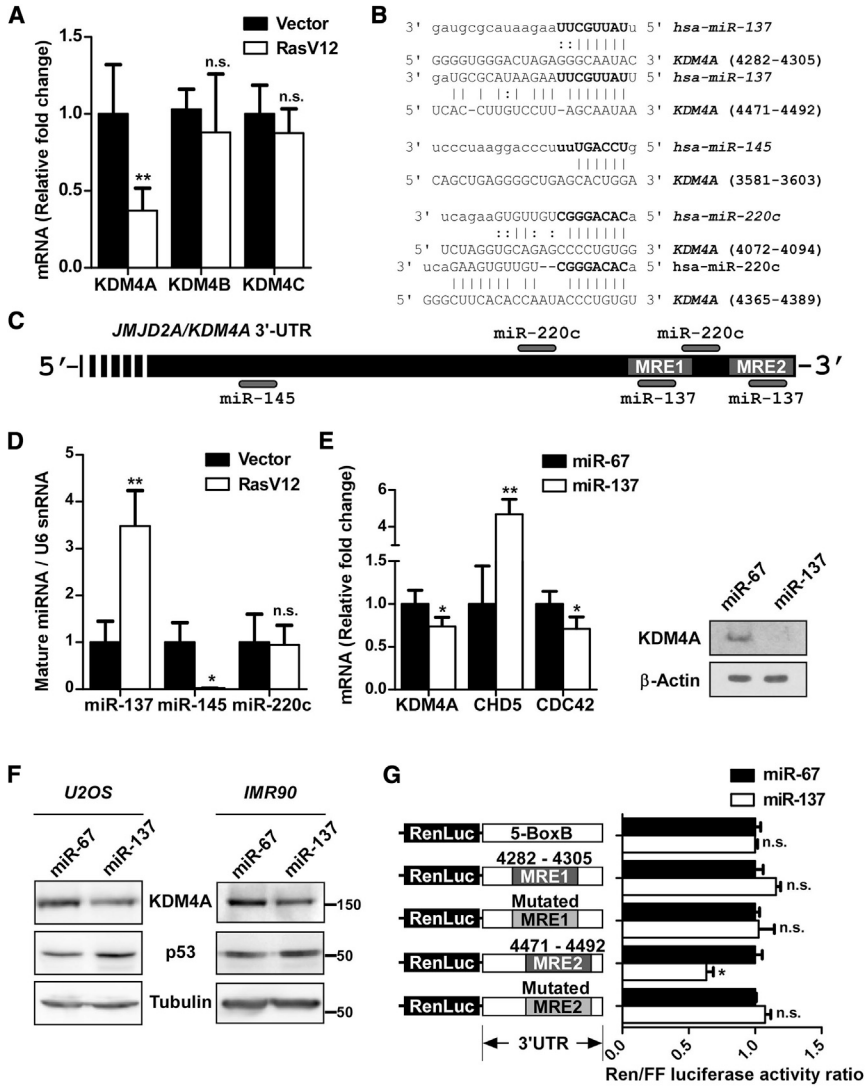

Figure 1. *KDM4A* Is a Target of Ras-Induced miR-137

(A) The mRNA expression levels of the *KDM4* family members were quantified by real-time qRT-PCR during Ras-induced senescence in IMR90 fibroblasts. The values were normalized to *GAPDH*. The significance was measured by the Student's t test and defined as $^{**}p < 0.01$ or n.s., non-significant (n = 3).

(B) The sequence of the miRNA-binding sites in the *KDM4A* 3′ UTR is shown, as predicted by miRANDA and TARGETSCAN algorithms.

(C) Schematic representations of the relative positions of putative miRNAs targeting the *KDM4A* 3′ UTR. The two miR-137 response elements (MREs) shown are not drawn to scale.

(D) Detection of the levels of miR-137, miR-145, and miR-220c by real-time qRT-PCR during Ras-induced senescence in IMR90 fibroblasts. The values were normalized to U6 small nuclear RNA (snRNA). The significance was measured by the Student's t test and defined as $^{*}p < 0.05$; $^{**}p < 0.01$; or n.s., non-significant (n = 3).

(E) Primary diploid human fibroblasts IMR90 fibroblasts were transfected twice with 20 nM miR-67 or miR-137 miRNA mimic within a 3-day interval and kept in culture for 8 days. (Left) The mRNA expression of *KDM4A*, *CHD5*, and *CDC42* was quantified by real-time qRT-PCR and normalized to the geometric mean of *ACTB* and *GAPDH*, as decribed by Vandesompele and colleagues (Vandesompele et al., 2002). The significance was measured by the Student's t test and defined as $^{*}p < 0.05$ or $^{**}p < 0.01$ (n = 3). (Right) Total cell lysates were immunoblotted with anti-KDM4A and anti-β-actin antibody was used to control for equivalent loading. Western blots are representative of three independent experiments.

(F) U2OS and IMR90 cells were transfected with either 100 nM miR-67 or miR-137 for 3 days. Total cell lysates were immunoblotted with anti-KDM4A, anti-p53 antibodies. Anti-α-tubulin antibody was used to control for equivalent loading. Western blots are representative of three independent experiments.

(G) HEK293T cells were transfected with 50 nM miR-67 or miR-137 miRNA mimic. The next day, cells were co-transfected with firefly luciferase plasmid and a *Renilla* luciferase reporter vector harboring either 5 BoxB sequences (5BoxB), wild-type human MRE1 or MRE2, or mutated versions. Data were normalized to the expression of the 5BoxB vector and expressed as the ratio of *Renilla*/firefly signals. Results shown are representative of three independent experiments. The significance was measured by the Student's t test and defined as $^{*}p < 0.05$ or n.s., non-significant.

See also Figures S1 and S2.

harboring either wild-type human MRE1 or MRE2 or mutated versions were generated and transfected in HEK293T cells along with miR-137 and a firefly luciferase plasmid to control for transfection efficiency; pCI-RL:MRE2 was sensitive to miR-137 expression, while pCI-RL:MRE1 was not (Figure 1G). Mutation of the MRE2 seed sequence rendered it insensitive to miR-137, whereas no change was observed with mutated MRE1 (Figure 1G). These findings suggest that miR-137 mainly targets MRE2 located from 4,471 to 4,492 (Figure 1G). *KDM4A* mRNA decay experiments using IMR90 cells stably expressing *H-Ras*^{V12} fused to an estrogen receptor ligand-binding domain (ER:RAS^{V12}) (Young et al., 2009) revealed that the half-life of the *KDM4A* mRNA is not affected by the establishment of the senescence phenotype (Figure S2B). These observations suggest that miR-137 negatively regulates KDM4A primarily through translational repression rather than mRNA levels, leading to the subsequent stimulation of the CHD5/p53 axis.

miR-137 Induces Senescence

We next postulated that miR-137 may promote senescence through the downregulation of KDM4A, and we evaluated this hypothesis by transfecting IMR90 normal human fibroblasts with an miR-137 mimic. A robust senescence response was observed upon transfection of miR-137 compared to miR-67-transfected cells, as assessed using senescence-associated β-galactosidase activity (SA-β-gal; Figure 2A; ~40% versus

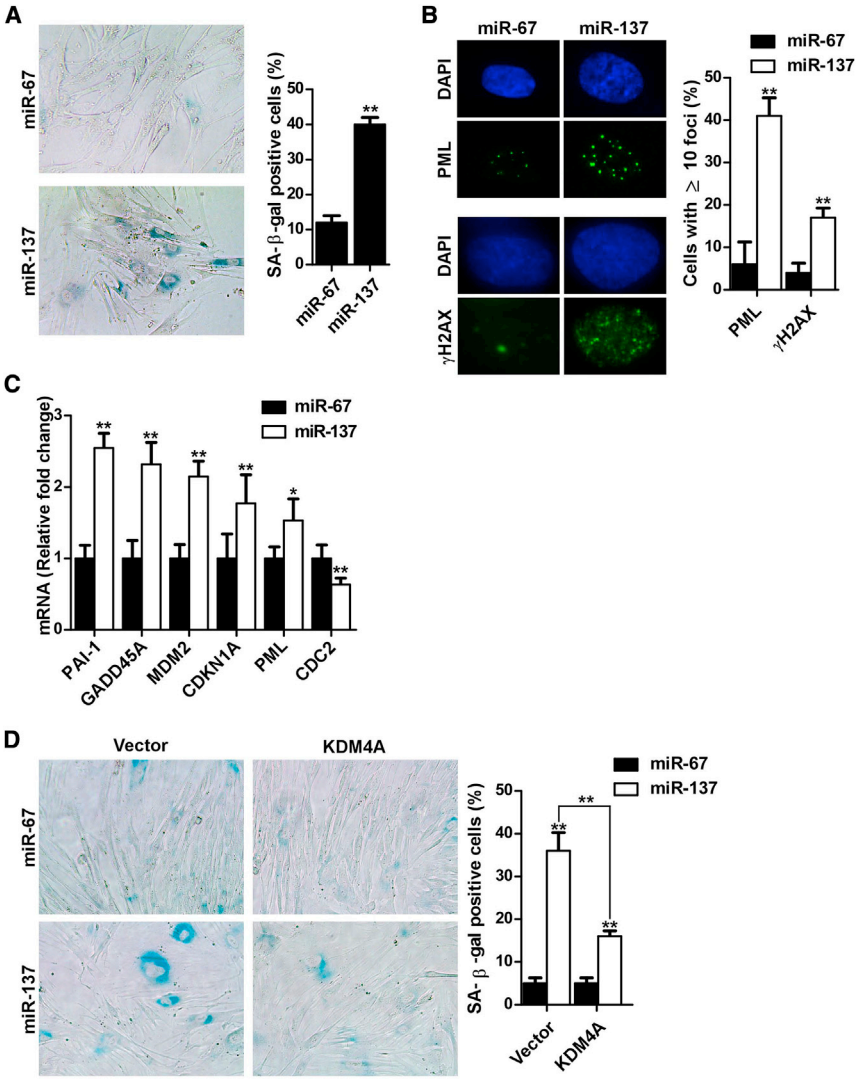

Figure 2. miR-137 Induces Cellular Senescence

(A) IMR90 fibroblasts were transfected with miRNA mimics and stained for SA-β-gal. Representative images are shown on the left and quantification is shown on the right. The mean percentage and SD of SA-β-gal-positive cells indicated in the right panel are representative of three independent experiments with >100 cells per experiment. The significance was measured by the Student's t test and defined as $^{**}p < 0.01$.

(B) Indirect immunoflurorescence of PML and γH2AX of cells prepared as in (A). The nuclei were counterstained with DAPI. Representative images are shown on the left and quantification is shown on the right. The mean percentage and SD of cells with more than ten foci indicated in the right panel are representative of three independent experiments, with >100 cells per experiment. The significance was measured by the Student's t test and defined as $^{**}p < 0.01$.

(C) Quantification by real-time qRT-PCR of the levels of p53 and E2F target genes of IMR90 fibroblasts described in (A). The values were normalized to the geometric mean of *ACTB* and *GAPDH*. The significance was measured by the Student's t test and defined as $^{*}p < 0.05$ or $^{**}p < 0.01$ (n = 3).

(D) IMR90 fibroblasts expressing empty vector, or FLAG-tagged KDM4A lacking the 3′ UTR, were transfected with miRNA mimic and stained for SA-β-gal. Representative images are shown on the left and quantification is shown on the right. The mean percentage and SD of SA-β-gal-positive cells indicated in the right panel are representative of three independent experiments with >100 cells per experiment. The significance was measured by the Student's t test and defined as $^{**}p < 0.01$.

~12%). Subsequently, an increase in the number of PML nuclear bodies and γH2AX foci, two known markers of cells undergoing cellular senescence (Ferbeyre et al., 2000; Mallette et al., 2007), also were observed in miR-137-expressing cells (Figure 2B).

We next examined whether miR-137 leads to the activation of the ARF/p53 and $p16^{INK4A}$/pRb pathways by qRT-PCR. The mRNA of several p53 targets, such as *PAI-1*, *GADD45A*, *MDM2*, *CDKN1A*, and *PML*, were increased in miR-137-transfected cells, but not in miR-67-transfected cells (Figure 2C). The expression of an E2F-responsive gene, *CDC2*, was significantly decreased upon miR-137 expression, consistent with the activation of the pRb pathway (Figure 2C). These observations show that miR-137 promotes premature senescence in normal human diploid fibroblasts and engages both ARF/p53 and $p16^{INK4A}$/pRb tumor suppressor pathways.

To test whether miR-137 induces senescence by depleting KDM4A, we reintroduced a miR-137-insensitive wild-type FLAG-tagged KDM4A variant into miR-137-transfected fibroblasts. The KDM4A expression vector carries the coding sequence, but it lacks the 3′ UTR containing the miR-137 complementary sequences and is, therefore, insensitive to miR-137. The expression of wild-type KDM4A partially rescued the miR-137-induced senescence phenotype, as assessed by SA-β-gal staining (Figure 2D; ~16% versus ~36%).

miR-137 Triggers Both ARF/p53- and $p16^{INK4A}$/pRb-Dependent Pathways

The establishment of senescence in normal human fibroblasts involves both the p53 and the $p16^{INK4A}$ tumor suppressor pathways (Ferbeyre et al., 2000; Mallette et al., 2007; Serrano et al., 1997). Since the expression of *KDM4A* could not completely rescue the senescence phenotype induced by miR-137 (Figure 2D), we proposed that miR-137 also could trigger senescence in a p53-independent manner, through the $p16^{INK4A}$ pathway. To verify which pathway(s) is targeted by miR-137, we transfected miR-137 mimic into fibroblasts where p53 or $p16^{INK4A}$ was depleted. Transfection of miR-137 mimic in sh_GFP control cells induced senescence in ~39% of the cell population, as shown by increased SA-β-gal-positive cells (Figure 3A). Interestingly, we observed that inhibition of either the

p53 or $p16^{INK4A}$ pathway separately was insufficient to completely block senescence induced by miR-137 (Figure 3A). This was further confirmed using additional hallmarks, such as increased PML bodies and γH2AX foci in sh_p16 or sh_p53 cells transfected with miR-137 (Figures 3B and 3C). A slight reduction in the number of PML bodies was observed in sh_p53-expressing cells as expected, since PML is a direct transcriptional target of p53 (de Stanchina et al., 2004). These findings suggest that ectopic expression of miR-137 does not exclusively activate p53 signaling via decreased *KDM4A* levels, but also engages the $p16^{INK4A}$ pathway.

To confirm that miR-137 triggers senescence by simultaneously activating the p53 and $p16^{INK4A}$ pathways, we expressed the human papilloma viral proteins E6 and E7 known to inhibit the p53 and pRb pathways, respectively (Shay et al., 1991). E6 promotes the proteasomal degradation of p53 (Maki et al., 1996; Scheffner et al., 1990), while E7 interferes with pRb by blocking its ability to repress E2F-dependent gene expression (Roman and Munger, 2013). Expression of human papilloma viral E6 and E7 in miR-137-transfected fibroblasts fully rescued the senescence phenotype, suggesting that miR-137 indeed relies on either the p53 or $p16^{INK4A}$ pathway to establish senescence (Figure 3D). Similarly, as shown in Figures 2D and 3A, miR-137-induced senescence was partially rescued in sh_p16- or KDM4A-expressing fibroblasts, while concomitant inhibition of $p16^{INK4A}$ and expression of *KDM4A* led to a complete block of miR-137-induced senescence (Figure 3E). These data confirm that miR-137 engages a tumor suppressor network involving p53 and pRb pathways to promote cellular senescence.

miR-137 Loss of Function Blocks Ras-Induced Senescence

To determine the functional significance of miR-137 induction during OIS, we used a lentiviral vector encoding an antisense sequence to mature miR-137 (miR-OFF-137) (Cheng et al., 2005) to inhibit its activity. We validated the inhibitory effect of miR-OFF-137 in IMR90 cells transfected with the MRE2 *Renilla* luciferase reporter. The presence of miR-OFF-137, but not miR-OFF-CTRL, led to an increase of ~20-fold in Renilla activity, consistent with decreased miR-137 function (Figure 4A). We then transduced miR-OFF-137 in ER:RAS^{V12}-expressing IMR90 fibroblasts, and we observed a senescence bypass after 9 days of Ras induction by OHT treatment, as revealed by a significantly lower number of SA-β-gal-positive cells and a characteristic flat, vacuolated cytoplasm compared to miR-OFF-CTRL-expressing cells (~15% versus ~53%; Figures 4B and 4C). Transcriptional activation of *CDKN1A* also was compromised in miR-137-inhibited cells after the induction of oncogenic Ras, as quantified by qRT-PCR, consistent with p53 activation (Figure 4D). These results show that inhibiting endogenous miR-137 expression in IMR90 cells prevents Ras-induced senescence.

DNA Damage Induces miR-137 Expression

DNA damage is an important instigator of cellular senescence in primary cells (Bartkova et al., 2006; Mallette et al., 2007). To define the mechanism regulating the expression of miR-137, we monitored its levels following DNA damage. Stimulation of the DNA damage response by doxorubicin led to a significant increase in miR-137 (Figure 5A) and a decrease in *KDM4A* mRNA levels (Figure 5B). As p53 transcriptional activity is stimulated after DNA damage, we next examined whether expression of miR-137 required p53. IMR90 cells expressing a small hairpin RNA (shRNA) targeting p53 exhibited decreased levels of miR-137, as well as the classical p53 target gene *CDKN1A*, although *GAPDH* expression levels were unaffected (Figure 5C). Taken together, these data suggest that miR-137 expression is stimulated by DNA damage and requires p53.

Pancreatic Cancer Exhibits Lower Levels of miR-137

K-Ras is activated by somatic mutations in a majority of human pancreatic cancers (Stephen et al., 2014). We have shown here that miR-137 is induced in normal cells expressing Ras^{V12} and following DNA damage (Figures 1D, S2A, and 5A), and it stimulates a tumor suppressor network involving the p53 and $p16^{INK4A}$ pathways. Therefore, we compared the relative levels of miR-137 in pancreatic tumor versus normal tissues. Analysis of tissue microarray expression data from Pei and coworkers (Pei et al., 2009), gathering gene expression profiles of 36 pancreatic tumor and 16 normal tissue samples (GEO: GSE16515), revealed significant decreased expression of miR-137 in pancreatic tumors compared to normal tissues, but not *KDM4A* mRNA levels (Figure 6A). We then compared the absolute amount of endogenous miR-137 in normal diploid IMR90 fibroblasts as well as in the *K-Ras*-mutated pancreatic cell line PANC-1. We observed that IMR90 fibroblasts contain ~55 copies of miR-137 per cell, while miR-137 was undetectable in PANC-1 cells (Figure S3). We therefore examined the relationship between the expression of miR-137 in tumor samples and *KDM4A* and *KDM4A*'s target genes (Mallette and Richard, 2012; Zhang et al., 2005). The expression of miR-137 in pancreatic tumor tissues correlated with levels of KDM4A-repressed genes *CHD5*, *ASCL2*, and *PANX2*, displaying coefficients of determination r^2 of 0.7810, 0.7874, and 0.4068, respectively (Figure 6B). The miR-137 expression also correlated with the *KDM4A*-stimulated target gene *PPIC* (Mallette and Richard, 2012), with a coefficient of determination r^2 of 0.2018 (Figure 6B). We did not observe a correlation between miR-137 and *KDM4A* mRNA (r^2 = 0.04611), nor did we observe a correlation between miR-137 and two of its own targets, *CDK6* and *CDC42* (r^2 of 0.01059 and 5.147E−5, respectively; Figure 6C). These findings suggest that there is a correlation between miR-137 and *KDM4A*'s target genes.

Restoration of miR-137 in Pancreatic Cancer Cells Causes Cellular Senescence

We have shown that oncogenic *Ras* signaling increased miR-137 levels and that it contributes to the establishment of the senescence program in normal human diploid cells. Since miR-137 expression is reduced in pancreatic tumors (Figures 6A and 6B), as well as absent in PANC-1 cells (Figure S3), we restored miR-137 expression in pancreatic tumor cells to determine if this can trigger cellular senescence. The expression of miR-137 in PANC-1 significantly decreased the growth rate (Figure 6D) and induced cellular senescence (Figure 6E).

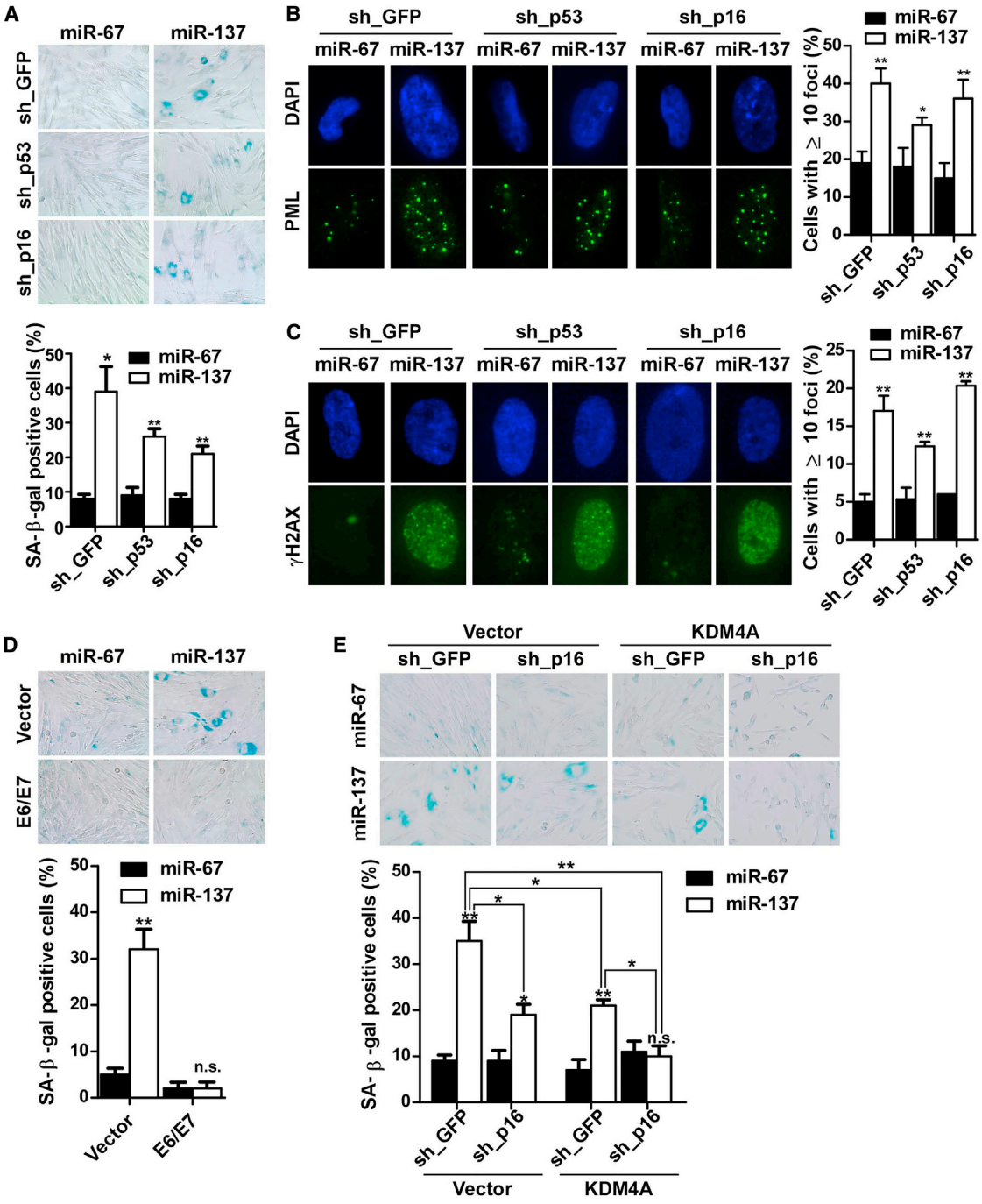

Figure 3. miR-137 Engages Both the p53 and p16^{INK4A} Tumor Suppressor Pathways

(A) IMR90 fibroblasts expressing sh_GFP, sh_p53, or sh_p16 were transfected with miRNA mimic and fixed for SA-β-gal staining. Representative images are depicted in the top panel and the quantification is below. The mean percentage and SD of SA-β-gal-positive cells indicated in the bottom panel are representative of three independent experiments with >100 cells per experiment. The significance was measured by the Student's t test and defined as $^*p < 0.05$ or $^{**}p < 0.01$.

(B and C) Indirect immunofluorescence against PML bodies or γH2AX foci in cells as prepared in (A). The nuclei were counterstained with DAPI. Representative images are shown on the left and quantification is shown on the right. The mean percentage and SD of cells with more than ten foci indicated in the right panel are representative of three independent experiments and expressed as SD of the mean, with >100 cells per experiment. The significance was measured by the Student's t test and defined as $^*p < 0.05$ or $^{**}p < 0.01$.

(D) IMR90 fibroblasts infected with empty or E6/E7-expressing vector were transfected with miRNA mimic and stained for SA-β-gal. Representative images are depicted in the top panel and the quantification is below. The mean percentage and SD of SA-β-gal-positive cells indicated on the bottom panel are

(legend continued on next page)

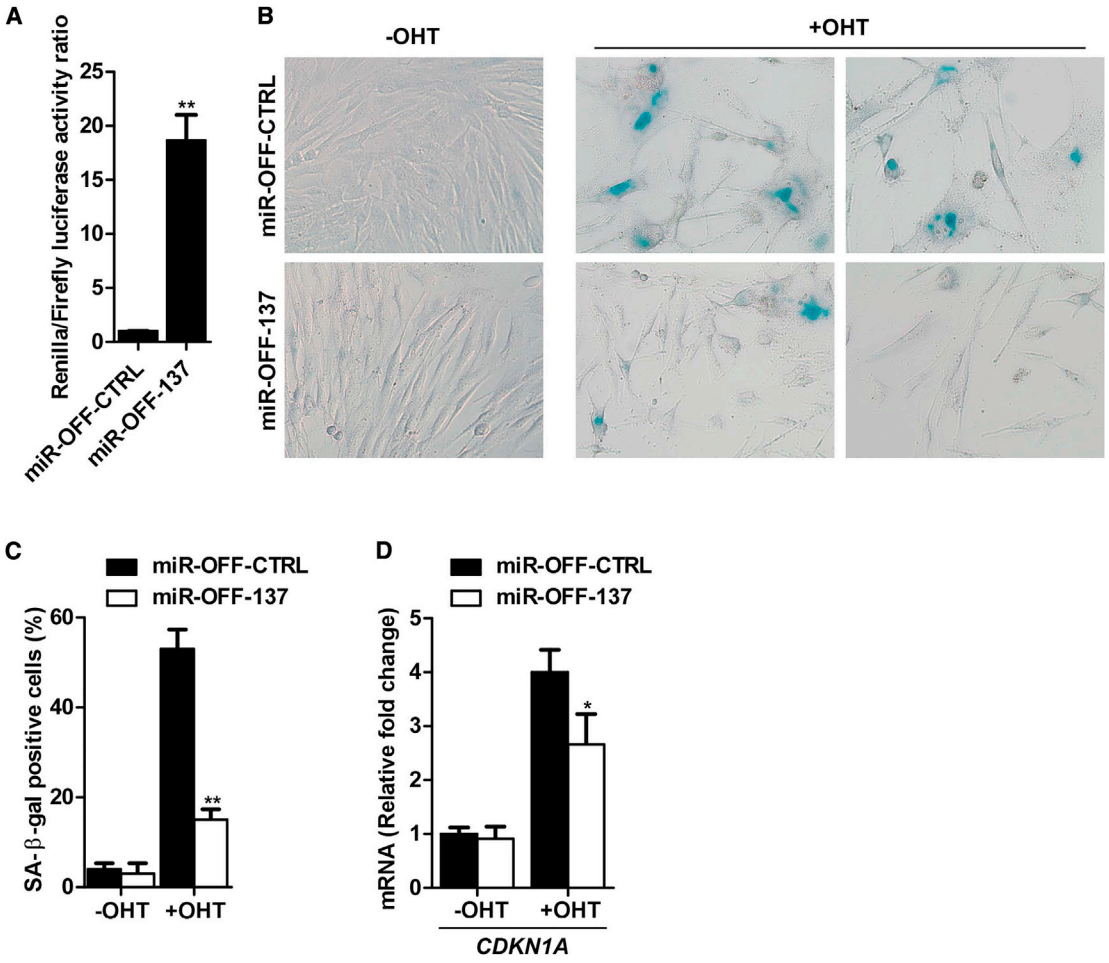

Figure 4. miR-137 Loss of Function Blocks Ras-Induced Senescence

(A) IMR90 fibroblasts were transduced with miR-OFF-CTRL or miR-OFF-137 inhibitor vector and transfected either with 5BoxB or MRE2 *Renilla* luciferase reporter described in Figure 1G. Firefly luciferase vector was used as a transfection control. Data were normalized to the expression of the 5BoxB vector and expressed as the ratio of *Renilla*/firefly signals. Results shown are representative of four independent experiments. The significance was measured by the Student's t test and defined as $^{**}p < 0.01$.

(B) IMR90 fibroblasts co-expressing ER:RAS^{V12} and miR-OFF-CTRL or miR-OFF-137 inhibitor vector were either supplemented with ethanol or 100 nM OHT for 9 days. Cells were fixed for SA-β-gal staining. Representative images of three independent experiments are shown.

(C) Quantification of SA-β-gal-positive cells in (B). The mean percentage and SD of SA-β-gal-positive cells indicated on the right panel are representative of three independent experiments with >100 cells per experiment. The significance was measured by the Student's t test and defined as $^{**}p < 0.01$.

(D) Quantification by real-time qRT-PCR of the levels of *CDKN1A* in cells described in (B). The values were normalized to the geometric mean of *ACTB* and *GAPDH*. The significance was measured by the Student's t test and defined as $^{*}p < 0.05$ (n = 3).

Comparable results were obtained with siRNA-mediated knockdown of *KDM4A* in PANC-1 cells (Figures S4A and S4B), suggesting the possible contribution of KDM4A depletion in triggering senescence of PANC-1 cells. These observations show that miR-137-induced senescence can be restored in PANC-1, thus blocking their proliferation.

DISCUSSION

In this paper, we describe the ability of miR-137 to induce cellular senescence. miR-137 levels are increased during OIS and in response to DNA damage. Ectopic expression of miR-137 led to a cell-cycle arrest phenotype associated with the hallmark

representative of three independent experiments with >100 cells per experiment. The significance was measured by the Student's t test and defined as $^{**}p < 0.01$ or n.s., non-significant.

(E) IMR90 fibroblasts co-expressing sh_GFP or sh_p16 and empty vector or FLAG-tagged-KDM4A were transfected with miRNA mimic and stained for SA-β-gal. Representative images are depicted in the top panel and the quantification is below. The mean percentage and SD of SA-β-gal-positive cells indicated on the bottom panel are representative of three independent experiments with >100 cells per experiment. The significance was measured by the Student's t test and defined as $^{*}p < 0.05$; $^{**}p < 0.01$; or n.s., non-significant.

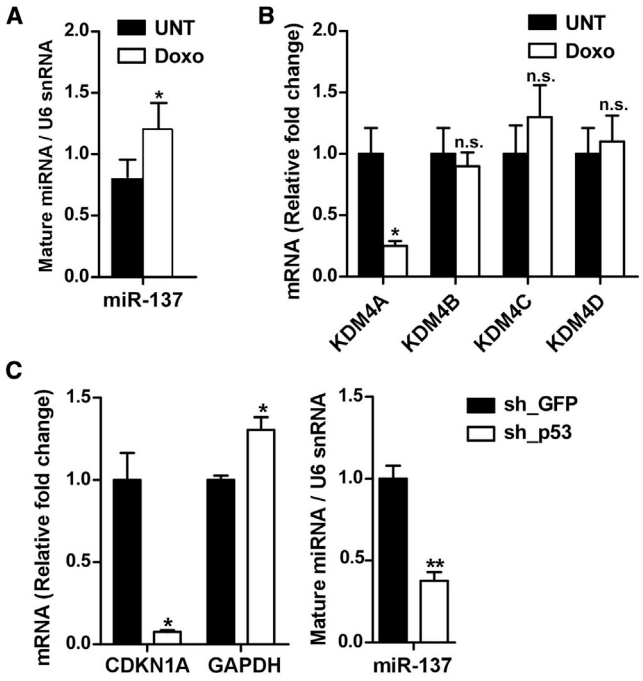

Figure 5. DNA Damage Induces miR-137

(A) Quantification by real-time qRT-PCR of the levels of miR-137 after 16-hr treatment with 1 μM doxorubicin of U2OS cells. The values were normalized to U6 snRNA. The significance was measured by the Student's t test and defined as *$p < 0.05$ ($n = 3$).

(B) The mRNA expression levels of the *KDM4* family members quantified by real-time qRT-PCR during DNA damage response from cells described in (A). The values were normalized to *ACTB* mRNA. The significance was measured by the Student's t test and defined as *$p < 0.05$ or n.s., non-significant ($n = 3$).

(C) RNA from IMR90 fibroblasts infected with either sh_GFP- or sh_p53-expressing vector was extracted and analyzed by real-time qRT-PCR. mRNA levels of *CDKN1A* and *GAPDH* were normalized to *ACTB*, while mature miR-137 levels were normalized to U6 snRNA. The significance was measured by the Student's t test and defined as *$p < 0.05$ or **$p < 0.01$ ($n = 3$).

of premature cellular senescence. We demonstrate that miR-137 engages both ARF/p53 and $p16^{INK4A}$/pRb pathways to promote cellular senescence, and we have identified the mRNA of the *KDM4A* lysine demethylase as an miR-137 target. KDM4A previously was shown to decrease during OIS and its restoration allowed bypass of cellular senescence (Mallette and Richard, 2012). We now show that downregulation of *KDM4A* by miR-137 activates the CHD5/p53 tumor suppressor pathway. In addition, expression of an miRNA-insensitive *KDM4A* partially rescued miR-137-induced senescence, while a complete rescue was achieved with the concomitant expression of KDM4A and depletion of $p16^{INK4A}$, consistent with miR-137 engaging both ARF/p53 and $p16^{INK4A}$/pRb pathways. Inhibition of endogenous miR-137 using an miRNA sponge in IMR90 severely compromised the OIS response and engendered a significant decrease of *CDKN1A* expression, thus confirming the contribution of miR-137 in the activation of p53 and establishment of cellular senescence. In human pancreatic tumors, we show that the expression of three transcriptional targets repressed by KDM4A, *CHD5*, *ASCL2*, and *PANX2*, correlated with miR-137 expression levels. This observation suggests that miR-137, by decreasing KDM4A levels, relieved KDM4A-mediated repression on these genes. Ectopic expression of miR-137 in pancreatic cancer cell line PANC-1 halted cell proliferation and induced cellular senescence, a cellular response also observed upon the depletion of KDM4A. These findings suggest that increasing miR-137 in pancreatic cancer might be of therapeutic significance.

Reduced expression levels of mature miR-137 has been reported in many tumor types including glioblastoma (Chen et al., 2012) and ovarian cancer (Guo et al., 2013), and also *Ras*-driven colorectal cancer (Chen et al., 2013), non-small cell lung carcinoma (Zhang et al., 2015), and prostate cancer (Nilsson et al., 2015). Furthermore, miR-137 was shown to reduce invasion while increasing sensitivity to chemotherapy in pancreatic cancer (Xiao et al., 2014). We now define the molecular mechanism of action of miR-137. In this respect, we have defined herein the molecular underpinnings by showing that miR-137 stimulates a tumor suppressor network engaging both ARF/p53 and $p16^{INK4A}$/pRb pathways to promote cellular senescence in pancreatic cancer cells. Taken together, our data also suggest that the ability of miR-137 to induce senescence may be relevant to many cancer types.

Activation of the DNA damage response is known to stimulate the maturation of specific miRNAs (Chowdhury et al., 2013). We show that the expression of miR-137 is induced by DNA damage, and further experimentation is required to define whether miR-137 is a direct target of p53. Attempts to identify chromatin-bound p53 at putative p53 response elements in the miR-137 upstream region by ChIP were unsuccessful (data not shown). It is possible that we have not identified the appropriate p53-binding site. p53 has been shown to stimulate the maturation of numerous miRNAs (Suzuki et al., 2009), and this also may be a mechanism by which miR-137 is regulated by p53. Thus, we have uncovered a mechanism whereby miR-137 and p53 promote each other's activation in a positive feedback loop during the DNA damage response and following oncogenic stress (see model Figure 7).

PDAC is the most frequent form of pancreatic cancer (~90% of the cases), is highly aggressive, and exhibits a very poor 5-year survival rate (<5%) (Bryant et al., 2014; Eser et al., 2014). Activating *K-Ras* mutations is recognized as a primary determinant in the initiation of pancreatic intraepithelial neoplasia (PanIN) (Eser et al., 2014), however, progression from low-grade PanIN to PDAC often requires the chronological disruption of the *INK4A/ARF* tumor suppressor locus followed by p53 inactivation (Hezel et al., 2006), leading to genomic instability and tumor progression (Bryant et al., 2014; Hezel et al., 2006). miR-137 expression is decreased in pancreatic tumors, and its restoration in PANC-1 cells induced cellular senescence response and growth inhibition. Accordingly, downstream miR-137 signaling seems intact and functional in pancreatic cancers. Additionally, bypass of OIS observed upon miR-137 loss of function greatly supports the notion that the loss of miR-137 is an early event driving pancreatic tumorigenesis in cooperation with activated Ras.

We observed that miR-137 levels are lower in a pancreatic tumor tissue cohort versus normal tissues. miR-137 expression correlated with levels of KDM4A downstream negative targets

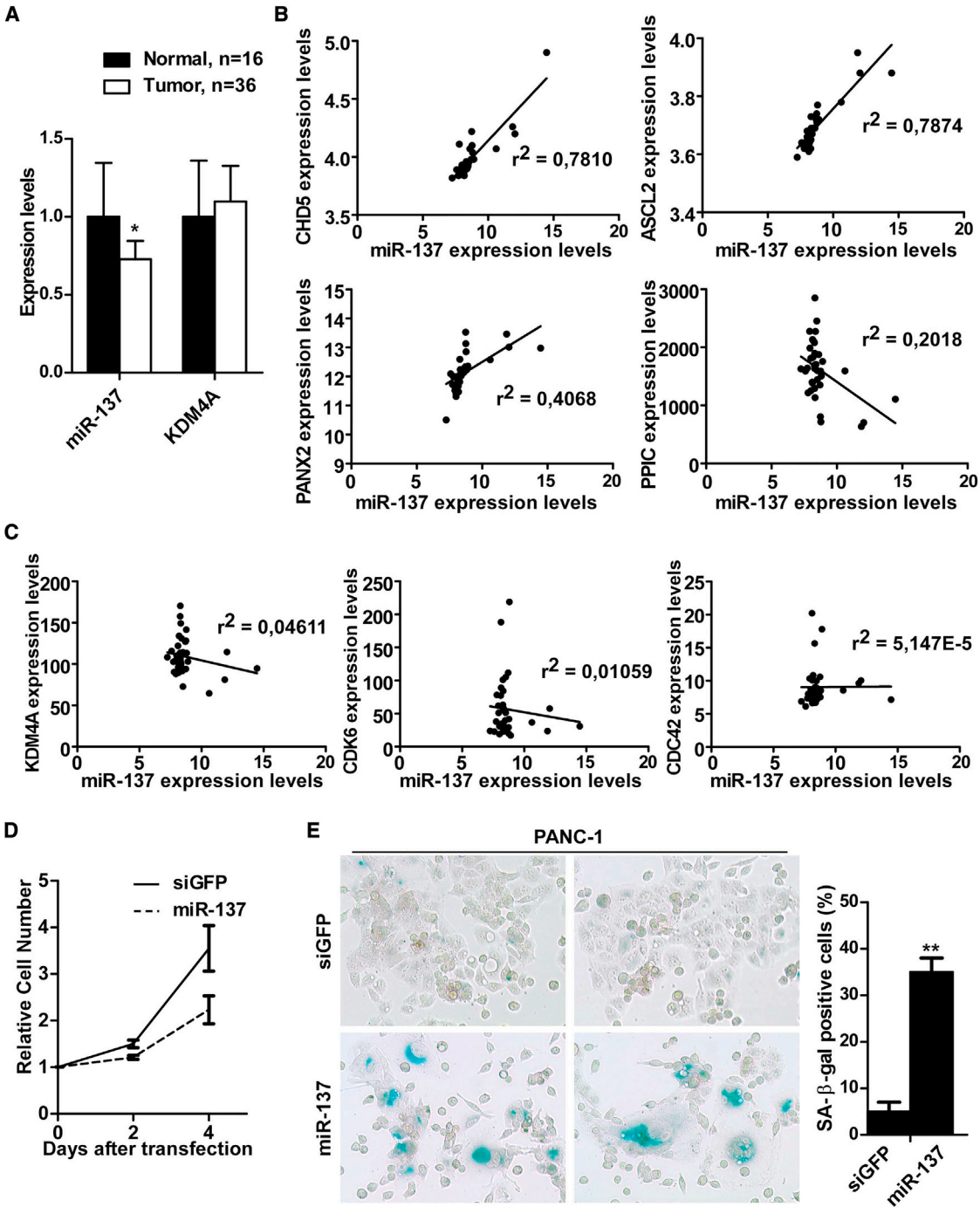

Figure 6. Restoration of miR-137 in Pancreatic Cancer Cells Induced Premature Senescence

(A) Levels of miR-137 and the KDM4A mRNA in normal and pancreatic tumor tissues were obtained from Affymetrix Human Genome U133 Plus 2.0 Array data. The significance was measured by the Student's t test and defined as *$p < 0.05$.

(B) Scatterplot showing correlation between the relative expression of endogenous miR-137 levels and *KDM4A* negative mRNA targets *CHD5*, *ASCL2*, and *PANX2* or *KDM4A*-positive target *PPIC* from the tumor samples described in (A). The coefficient of determination r^2 is shown adjacent to the linear regression curve.

(C) *KDM4A*, *CDK6*, and *CDC42* were plotted as described in (B). The coefficient of determination r^2 is shown adjacent to the linear regression curve.

(D) Growth curve of PANC-1 cells transfected with 50 nM siGFP or miR-137 mimic is shown.

(legend continued on next page)

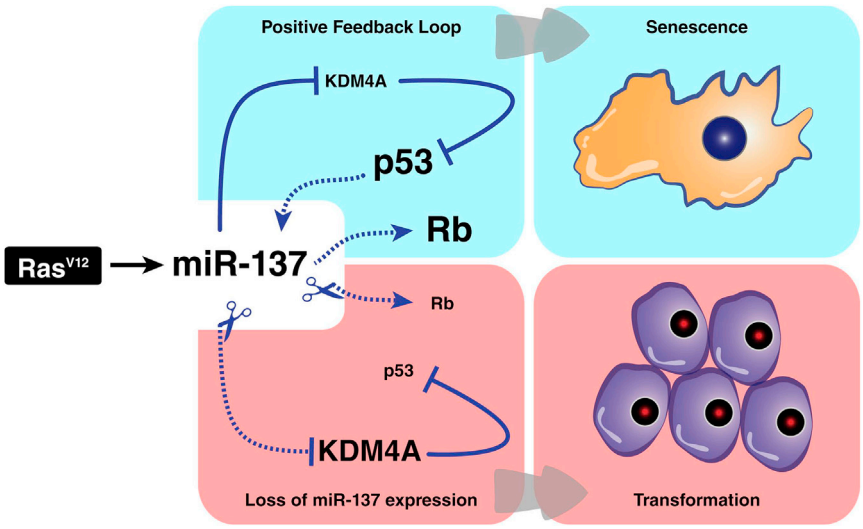

Figure 7. Model of Senescence Induction by miR-137 following OIS

In normal cells, increased levels of miR-137 upon oncogenic Ras triggers the p53 and Rb pathways to promote cellular senescence. Inhibition of KDM4A by miR-137 stabilizes p53, which in turn stimulates miR-137 in a positive feedback loop. The loss of miR-137 impairs OIS and cooperates with Ras to bypass senescence, promoting tumorigenesis. A dashed line is used to show that miR-137 is a putative p53 target.

CHD5, *ASCL2*, and *PANX2* and also with KDM4A positively modulated target *PPIC*. The levels of mRNAs for *KDM4A* in these pancreatic cancer samples did not correlate with decreased miR-137 levels. Although miR-137 might primarily regulate *KDM4A* mRNA translation rather than mRNA degradation, it is possible that there are other factors that preclude us from observing *KDM4A* mRNA decay, such as elevated levels of steady-state mRNAs. Moreover, we observed that the half-life of the *KDM4A* mRNA in cycling fibroblasts is similar to senescent fibroblasts induced by Ras^{V12}. This may be explained by the fact that miRNA-mediated silencing is not solely the result of mRNA decay, but also can be attributed to 5′ cap-dependent translation inhibition (Filipowicz and Sonenberg, 2015). Thus, the transcriptional analysis of *KDM4A* downstream targets constituted a more informative measure of *KDM4A* activity than *KDM4A* mRNA levels.

It is important to consider endogenous miRNA expression levels when studying miRNA-mediated translation inhibition. miR-137 is annotated with 54 reads per million in the latest version of miRBase database (http://www.mirbase.org/). Other low-copy miRNAs, such as the miR-34 family (e.g., miR-34b annotated with 294 reads on miRBase), have been shown to induce senescence, and their loss of expression is a common feature in cancer (Hermeking, 2010).

Despite relatively low amounts of miR-137, its >5-fold increase observed in our RasV12-induced senescence model (Figure S2A) reaches the same levels as miR-34. In addition, inhibition of miR-137 endogenous activity significantly impaired the OIS response (Figure 4), and its expression was undetected in pancreatic cancer cells. These results are consistent with our findings that miR-137 is lost in pancreatic cancer, and they reveal that miR-137 is a physiologically relevant mediator of OIS.

miR-137 stimulates cellular senescence by engaging the $p16^{INK4A}$/pRb and the ARF/p53 pathways independently (Figures 2C and 3A). The partial contribution of KDM4A in rescuing miR-137-induced senescence (Figure 2D) implies that there are other effectors of miR-137 involved in promoting senescence. miR-137 is known to target cyclin-dependent kinase *CDK6* and the Rho-GTPase family member *CDC42* (Liu et al., 2011; Zhu et al., 2013). CDK6 forms a complex with cyclin D to phosphorylate pRb and release it from E2F-dependent genes, thus permitting S phase entry (Choi and Anders, 2014). CDC42 controls cell-cycle progression by stimulating cyclin D expression (Welsh et al., 2001), and it cooperates with oncogenic *Ras* during transformation (Qiu et al., 1997). Thus, miR-137 might regulate the $p16^{INK4A}$/pRb pathway at multiple levels, possibly through downregulation of *CDK6* and *CDC42*. On the other hand, miR-137 dampens *KDM4A* activity to stimulate the p53 pathway in a positive feedback loop and also triggers the $p16^{INK4A}$/pRb pathway, which leads to cell-cycle arrest and senescence (Figure 7). *KDM4A* mRNA is a main target of miR-137 in the ARF/p53 pathway, since the concomitant restoration of miR-137-resistant *KDM4A* in $p16^{INK4A}$-depleted cells leads to a complete bypass of senescence (Figure 3E).

miR-137 has been shown to modulate various cell-cycle regulators in Ras-dependent malignancies (Chen et al., 2012; Guo et al., 2013; Liu et al., 2011; Zhang et al., 2015). Recently, miR-137 was shown to regulate prostate and breast cancer cells' proliferation by targeting a network of histone demethylases, including *KDM1A*, *KDM4A*, *KDM5*, and *KDM7A* (Denis et al., 2016; Nilsson et al., 2015), although the molecular mechanism and physiological relevance of these observations remains to be defined. Our findings provide the molecular evidence that miR-137 regulation of KDM4A promotes cellular senescence in pancreatic cancer, further supporting the tumor suppressor activity of miR-137. We provide data that miR-137 not only restrains proliferation, but also is likely an intermediate that bridges the gap between oncogenic stress signals and the senescence response to ultimately counter cellular transformation (Figure 7).

(E) PANC-1 cells described in (D) were fixed 8 days after transfection and stained for SA-β-gal. The mean percentage and SD of SA-β-gal-positive cells indicated on the right panel are representative of two independent experiments with >100 cells per experiment. The significance was measured by the Student's t test and defined as $^{**}p < 0.01$.

See also Figures S3 and S4.

Since miR-137 promotes cellular senescence and forestalls tumorigenesis, it would be of importance to identify other mechanisms by which miR-137 might block transformation in vivo. Recently, miRNAs also were found to participate in transcriptional gene silencing, specifically in the case of proliferation-promoting genes during senescence (Benhamed et al., 2012). Of note, miR-137 has been found enriched in heterochromatin during OIS (Benhamed et al., 2012), suggesting that miR-137 also may regulate gene expression at the transcriptional level.

In view of the primary role of activated oncogenic *Ras* in human cancers, many strategies have been employed to inhibit the *Ras* pathway (Samatar and Poulikakos, 2014). One current approach involves targeting the downstream MAP kinase effectors MEK and ERK (Sullivan and Flaherty, 2013). However, the induction of senescence following *Ras* activation also has proven to be an effective intrinsic tumor suppression mechanism (Braig et al., 2005; Chen et al., 2005; Collado et al., 2005; Michaloglou et al., 2005). As such our finding that miR-137 is an effector of *Ras* during OIS provides additional insights for inducing tumor suppressor networks in pancreatic cancer.

EXPERIMENTAL PROCEDURES

Western Blot Analysis

Cell were lysed in 20 mM Tris-HCl (pH 7.5), 150 mM NaCl, 1 mM EDTA, 1 mM EGTA, and 1% Triton X-100 with Complete EDTA-free protease inhibitors (Roche) and sonicated on ice three times 10 s. Cell extracts were separated by SDS-PAGE and transferred to a nitrocellulose membrane (Bio-Rad) for immunoblotting. Primary antibodies used were the following: anti-α-tubulin (B-5-1-2, Sigma, 1:50,000), anti-β-actin (A5441, Sigma, 1:5,000), anti-KDM4A (75-189, clone N154/32, Neuromab, 1:1,000), and anti-p53 horseradish peroxidase (HRP) conjugated (HAF1355, R&D Systems, 1:5,000). Goat anti-mouse or goat anti-rabbit IgG antibodies conjugated to HRP were purchased from Sigma-Aldrich and detected using the enhanced chemiluminescence (ECL) detection kit (DuPont).

Cell Culture, Retroviral Infections, and siRNA and miRNA Transfections

Human fetal lung fibroblasts IMR90 (Coriell), HEK293T embryonic kidney (ATCC), and osteosarcoma cells U2OS (ATCC) were cultured in DMEM, and pancreatic cancer cell line PANC-1 (ATCC) was cultured in RPMI medium supplemented with 10% fetal bovine serum (FBS), 1 mM sodium pyruvate, and antibiotics. Retroviral infection procedures and vectors used (pLPC-puro and pLPC-puro FLAG-KDM4A) were described previously (Mallette et al., 2012). pLXSN and pLXSN-E6/E7 vectors were described previously (Mallette et al., 2007). pLenti-III-miR-Off-Blank (miR-OFF-Ctrl) and pLenti-III-miR-Off-137 (miR-OFF-137) miRNA inhibitor lentiviral vectors were purchased from Applied Biological Materials. The OHT-inducible RasV12 vector pLNCX2-neo (ER:RasV12) was a kind gift from Dr. Masashi Narita. Cells expressing pLNCX2-neo (ER:RasV12) were subcultured in phenol red-free DMEM medium and renewed with fresh OHT every 2–3 days. Transfection of plasmid DNA in HEK293T cells was performed using Lipofectamine 2000 (Invitrogen), and transfections in IMR90 fibroblasts were carried out using polyethylenimine (PEI, Sigma) according to the manufacturer's instructions. For miR-137-induced senescence experiments, we performed two transfections with a 4-day interval to ensure high levels of miRNA mimic during the whole assay. For DNA damage induction, cells were either left untreated or incubated with 500 nM doxorubicin for 16 hr. The list of siRNAs and miRNAs used is provided in the Supplemental Experimental Procedures.

Luciferase Reporter Assay

HEK293T cells were transfected with 50 nM miRNA mimic. The day after, the cells were co-transfected with the pMIR REPORT *Photinus pyralis* (firefly) luciferase vector (Life Technologies) containing no 3′ UTR as a transfection control and the pCI-RL *Renilla reniformis* (*Renilla*) reporters. For the reporter assay in IMR90 fibroblasts, the transfections were carried out using PEI. The next day, cells were lysed in passive lysis buffer and assayed using the Dual-Luciferase Reporter Assay System (Promega) according to the manufacturer's instructions. Firefly and *Renilla* luminescence signals were read using the GloMax 20/20 luminometer (Promega) with an integration time of 10 s for each signal. For the construction of the pCI-RLreporter vectors, 150 bp derived from the *KDM4A* mRNA 3′ UTR harboring wild-type MREs (miR-137 Seed 1 (MRE1): region 4,209–4,358, seed sequence 5′-GGG GTG GGA CTA GAG GGC AAT AC-3′; miR-137 Seed 2 (MRE2): region 4,359–4,508, seed sequence 5′-CAT CAC CTT GTC CTT AGC AAT AA-3′) or mutated MREs were subcloned between the *NheI* and *XbaI* sites of the pCI-RL-5BoxB vector (Pillai et al., 2004). For the mutated reporters, seed sequences were as follows: mutated MRE1, 5′-GGG GTG GGA CTA GAT TCG TTA TC; and mutated MRE2, 5′-CAT CAC CTT GTC CTT TCG TTA TA-3′. The pCI-RL-5BoxB vector was a kind gift from Dr. Mark R. Fabian.

SA-β-gal Activity

Cells were stained for SA-β-gal activity as previously described (Mallette et al., 2007). Briefly, IMR90 and PANC-1 cells were fixed with 0.5% glutaraldehyde in PBS for 15 min at room temperature. Fixed cells were washed and stained at 37°C. The staining solution was prepared fresh from potassium ferrocyanide and potassium ferricyanide salt, X-Gal, and $MgCl_2$ in PBS (pH 6.0).

Immunofluorescence

Immunostaining was performed essentially as described previously (Neault et al., 2012). Briefly, cells were grown on glass coverslips, fixed with 4% paraformaldehyde, and permeabilized with 0.2% Triton X-100. Cells were then incubated with anti-PML (PG-M3, Santa Cruz Biotechnology, 1:200) or anti γ-H2AX antibody followed by staining with an Alexa Fluor 488-conjugated goat anti-mouse secondary antibody and DAPI staining to detect nuclei. Coverslips were mounted with Immuno-Mount (Thermo Scientific). Images were taken using Zeiss M1 and Olympus BX 53 fluorescence microscopes.

SUPPLEMENTAL INFORMATION

Supplemental Information includes Supplemental Experimental Procedures and four figures and can be found with this article online at http://dx.doi.org/10.1016/j.celrep.2016.01.068.

AUTHOR CONTRIBUTIONS

M.N. and F.A.M. designed and performed experiments. M.N. analyzed the results and performed the statistical analyses. M.N., F.A.M., and S.R. conceived the study and wrote and edited the manuscript. F.A.M. and S.R. secured funding.

ACKNOWLEDGMENTS

We thank Dr. Elliot Drobetsky for critical reading of the manuscript. We thank Marie-Anne Germain for technical assistance and members of the S.R. and F.A.M. laboratories for helpful discussions. This work was funded by the Canadian Institutes of Health Research (CIHR) grants (MOP-93811 to S.R. and MOP-133442 to F.A.M.). M.N. is funded by a Ph.D. studentship from the Fonds de Recherche du Québec - Santé (FRQ-S). F.A.M. is a Junior 1 Research Scholar of the FRQ-S.

Received: May 14, 2015
Revised: December 10, 2015
Accepted: January 22, 2016
Published: February 18, 2016

REFERENCES

Bagchi, A., Papazoglu, C., Wu, Y., Capurso, D., Brodt, M., Francis, D., Bredel, M., Vogel, H., and Mills, A.A. (2007). CHD5 is a tumor suppressor at human 1p36. Cell *128*, 459–475.

Bartkova, J., Rezaei, N., Liontos, M., Karakaidos, P., Kletsas, D., Issaeva, N., Vassiliou, L.V., Kolettas, E., Niforou, K., Zoumpourlis, V.C., et al. (2006). Oncogene-induced senescence is part of the tumorigenesis barrier imposed by DNA damage checkpoints. Nature *444*, 633–637.

Bemis, L.T., Chen, R., Amato, C.M., Classen, E.H., Robinson, S.E., Coffey, D.G., Erickson, P.F., Shellman, Y.G., and Robinson, W.A. (2008). MicroRNA-137 targets microphthalmia-associated transcription factor in melanoma cell lines. Cancer Res. *68*, 1362–1368.

Benhamed, M., Herbig, U., Ye, T., Dejean, A., and Bischof, O. (2012). Senescence is an endogenous trigger for microRNA-directed transcriptional gene silencing in human cells. Nat. Cell Biol. *14*, 266–275.

Black, J.C., Manning, A.L., Van Rechem, C., Kim, J., Ladd, B., Cho, J., Pineda, C.M., Murphy, N., Daniels, D.L., Montagna, C., et al. (2013). KDM4A lysine demethylase induces site-specific copy gain and rereplication of regions amplified in tumors. Cell *154*, 541–555.

Braig, M., Lee, S., Loddenkemper, C., Rudolph, C., Peters, A.H., Schlegelberger, B., Stein, H., Dörken, B., Jenuwein, T., and Schmitt, C.A. (2005). Oncogene-induced senescence as an initial barrier in lymphoma development. Nature *436*, 660–665.

Bryant, K.L., Mancias, J.D., Kimmelman, A.C., and Der, C.J. (2014). KRAS: feeding pancreatic cancer proliferation. Trends Biochem. Sci. *39*, 91–100.

Chellappan, S.P., Hiebert, S., Mudryj, M., Horowitz, J.M., and Nevins, J.R. (1991). The E2F transcription factor is a cellular target for the RB protein. Cell *65*, 1053–1061.

Chen, Z., Trotman, L.C., Shaffer, D., Lin, H.K., Dotan, Z.A., Niki, M., Koutcher, J.A., Scher, H.I., Ludwig, T., Gerald, W., et al. (2005). Crucial role of p53-dependent cellular senescence in suppression of Pten-deficient tumorigenesis. Nature *436*, 725–730.

Chen, L., Wang, X., Wang, H., Li, Y., Yan, W., Han, L., Zhang, K., Zhang, J., Wang, Y., Feng, Y., et al. (2012). miR-137 is frequently down-regulated in glioblastoma and is a negative regulator of Cox-2. Eur. J. Cancer *48*, 3104–3111.

Chen, D.L., Wang, D.S., Wu, W.J., Zeng, Z.L., Luo, H.Y., Qiu, M.Z., Ren, C., Zhang, D.S., Wang, Z.Q., Wang, F.H., et al. (2013). Overexpression of paxillin induced by miR-137 suppression promotes tumor progression and metastasis in colorectal cancer. Carcinogenesis *34*, 803–811.

Cheng, A.M., Byrom, M.W., Shelton, J., and Ford, L.P. (2005). Antisense inhibition of human miRNAs and indications for an involvement of miRNA in cell growth and apoptosis. Nucleic Acids Res. *33*, 1290–1297.

Chicas, A., Wang, X., Zhang, C., McCurrach, M., Zhao, Z., Mert, O., Dickins, R.A., Narita, M., Zhang, M., and Lowe, S.W. (2010). Dissecting the unique role of the retinoblastoma tumor suppressor during cellular senescence. Cancer Cell *17*, 376–387.

Choi, Y.J., and Anders, L. (2014). Signaling through cyclin D-dependent kinases. Oncogene *33*, 1890–1903.

Chowdhury, D., Choi, Y.E., and Brault, M.E. (2013). Charity begins at home: non-coding RNA functions in DNA repair. Nat. Rev. Mol. Cell Biol. *14*, 181–189.

Collado, M., Gil, J., Efeyan, A., Guerra, C., Schuhmacher, A.J., Barradas, M., Benguría, A., Zaballos, A., Flores, J.M., Barbacid, M., et al. (2005). Tumour biology: senescence in premalignant tumours. Nature *436*, 642.

de Stanchina, E., Querido, E., Narita, M., Davuluri, R.V., Pandolfi, P.P., Ferbeyre, G., and Lowe, S.W. (2004). PML is a direct p53 target that modulates p53 effector functions. Mol. Cell *13*, 523–535.

Denis, H., Van Grembergen, O., Delatte, B., Dedeurwaerder, S., Putmans, P., Calonne, E., Rothe, F., Sotiriou, C., Fuks, F., and Deplus, R. (2016). MicroRNAs regulate KDM5 histone demethylases in breast cancer cells. Mol. Biosyst. *12*, 404–413.

Dickins, R.A., Hemann, M.T., Zilfou, J.T., Simpson, D.R., Ibarra, I., Hannon, G.J., and Lowe, S.W. (2005). Probing tumor phenotypes using stable and regulated synthetic microRNA precursors. Nat. Genet. *37*, 1289–1295.

Enright, A.J., John, B., Gaul, U., Tuschl, T., Sander, C., and Marks, D.S. (2003). MicroRNA targets in Drosophila. Genome Biol. *5*, R1.

Eser, S., Schnieke, A., Schneider, G., and Saur, D. (2014). Oncogenic KRAS signalling in pancreatic cancer. Br. J. Cancer *111*, 817–822.

Feng, Z., Zhang, C., Wu, R., and Hu, W. (2011). Tumor suppressor p53 meets microRNAs. J. Mol. Cell Biol. *3*, 44–50.

Ferbeyre, G., de Stanchina, E., Querido, E., Baptiste, N., Prives, C., and Lowe, S.W. (2000). PML is induced by oncogenic ras and promotes premature senescence. Genes Dev. *14*, 2015–2027.

Filipowicz, W., and Sonenberg, N. (2015). The long unfinished march towards understanding microRNA-mediated repression. RNA *21*, 519–524.

Gan, Q., Huang, J., Zhou, R., Niu, J., Zhu, X., Wang, J., Zhang, Z., and Tong, T. (2008). PPARgamma accelerates cellular senescence by inducing p16INK4alpha expression in human diploid fibroblasts. J. Cell Sci. *121*, 2235–2245.

Guo, J., Xia, B., Meng, F., and Lou, G. (2013). miR-137 suppresses cell growth in ovarian cancer by targeting AEG-1. Biochem. Biophys. Res. Commun. *441*, 357–363.

Hermeking, H. (2010). The miR-34 family in cancer and apoptosis. Cell Death Differ. *17*, 193–199.

Hezel, A.F., Kimmelman, A.C., Stanger, B.Z., Bardeesy, N., and Depinho, R.A. (2006). Genetics and biology of pancreatic ductal adenocarcinoma. Genes Dev. *20*, 1218–1249.

Hong, L., Lai, M., Chen, M., Xie, C., Liao, R., Kang, Y.J., Xiao, C., Hu, W.Y., Han, J., and Sun, P. (2010). The miR-17-92 cluster of microRNAs confers tumorigenicity by inhibiting oncogene-induced senescence. Cancer Res. *70*, 8547–8557.

Iorio, M.V., Ferracin, M., Liu, C.G., Veronese, A., Spizzo, R., Sabbioni, S., Magri, E., Pedriali, M., Fabbri, M., Campiglio, M., et al. (2005). MicroRNA gene expression deregulation in human breast cancer. Cancer Res. *65*, 7065–7070.

Jin, J., Hu, H., Li, H.S., Yu, J., Xiao, Y., Brittain, G.C., Zou, Q., Cheng, X., Mallette, F.A., Watowich, S.S., and Sun, S.C. (2014). Noncanonical NF-κB pathway controls the production of type I interferons in antiviral innate immunity. Immunity *40*, 342–354.

Johnson, S.M., Grosshans, H., Shingara, J., Byrom, M., Jarvis, R., Cheng, A., Labourier, E., Reinert, K.L., Brown, D., and Slack, F.J. (2005). RAS is regulated by the let-7 microRNA family. Cell *120*, 635–647.

Kozaki, K., Imoto, I., Mogi, S., Omura, K., and Inazawa, J. (2008). Exploration of tumor-suppressive microRNAs silenced by DNA hypermethylation in oral cancer. Cancer Res. *68*, 2094–2105.

Kuilman, T., Michaloglou, C., Mooi, W.J., and Peeper, D.S. (2010). The essence of senescence. Genes Dev. *24*, 2463–2479.

Kunz, C., Pebler, S., Otte, J., and von der Ahe, D. (1995). Differential regulation of plasminogen activator and inhibitor gene transcription by the tumor suppressor p53. Nucleic Acids Res. *23*, 3710–3717.

Lewis, B.P., Shih, I.H., Jones-Rhoades, M.W., Bartel, D.P., and Burge, C.B. (2003). Prediction of mammalian microRNA targets. Cell *115*, 787–798.

Lin, A.W., Barradas, M., Stone, J.C., van Aelst, L., Serrano, M., and Lowe, S.W. (1998). Premature senescence involving p53 and p16 is activated in response to constitutive MEK/MAPK mitogenic signaling. Genes Dev. *12*, 3008–3019.

Liu, M., Lang, N., Qiu, M., Xu, F., Li, Q., Tang, Q., Chen, J., Chen, X., Zhang, S., Liu, Z., et al. (2011). miR-137 targets Cdc42 expression, induces cell cycle G1 arrest and inhibits invasion in colorectal cancer cells. Int. J. Cancer *128*, 1269–1279.

Lowe, S.W., and Sherr, C.J. (2003). Tumor suppression by Ink4a-Arf: progress and puzzles. Curr. Opin. Genet. Dev. *13*, 77–83.

Lowe, S.W., Cepero, E., and Evan, G. (2004). Intrinsic tumour suppression. Nature *432*, 307–315.

Maki, C.G., Huibregtse, J.M., and Howley, P.M. (1996). In vivo ubiquitination and proteasome-mediated degradation of p53(1). Cancer Res. *56*, 2649–2654.

Mallette, F.A., and Richard, S. (2012). JMJD2A promotes cellular transformation by blocking cellular senescence through transcriptional repression of the tumor suppressor CHD5. Cell Rep. *2*, 1233–1243.

Mallette, F.A., Gaumont-Leclerc, M.F., and Ferbeyre, G. (2007). The DNA damage signaling pathway is a critical mediator of oncogene-induced senescence. Genes Dev. *21*, 43–48.

Mallette, F.A., Mattiroli, F., Cui, G., Young, L.C., Hendzel, M.J., Mer, G., Sixma, T.K., and Richard, S. (2012). RNF8- and RNF168-dependent degradation of KDM4A/JMJD2A triggers 53BP1 recruitment to DNA damage sites. EMBO J. *31*, 1865–1878.

McConnell, B.B., Starborg, M., Brookes, S., and Peters, G. (1998). Inhibitors of cyclin-dependent kinases induce features of replicative senescence in early passage human diploid fibroblasts. Curr. Biol. *8*, 351–354.

Michaloglou, C., Vredeveld, L.C., Soengas, M.S., Denoyelle, C., Kuilman, T., van der Horst, C.M., Majoor, D.M., Shay, J.W., Mooi, W.J., and Peeper, D.S. (2005). BRAFE600-associated senescence-like cell cycle arrest of human naevi. Nature *436*, 720–724.

Moir, J.A., White, S.A., and Mann, J. (2014). Arrested development and the great escape–the role of cellular senescence in pancreatic cancer. Int. J. Biochem. Cell Biol. *57*, 142–148.

Neault, M., Mallette, F.A., Vogel, G., Michaud-Levesque, J., and Richard, S. (2012). Ablation of PRMT6 reveals a role as a negative transcriptional regulator of the p53 tumor suppressor. Nucleic Acids Res. *40*, 9513–9521.

Nevins, J.R., Chellappan, S.P., Mudryj, M., Hiebert, S., Devoto, S., Horowitz, J., Hunter, T., and Pines, J. (1991). E2F transcription factor is a target for the RB protein and the cyclin A protein. Cold Spring Harb. Symp. Quant. Biol. *56*, 157–162.

Nilsson, E.M., Laursen, K.B., Whitchurch, J., McWilliam, A., Ødum, N., Persson, J.L., Heery, D.M., Gudas, L.J., and Mongan, N.P. (2015). MiR137 is an androgen regulated repressor of an extended network of transcriptional coregulators. Oncotarget *6*, 35710–35725.

Pearson, M., Carbone, R., Sebastiani, C., Cioce, M., Fagioli, M., Saito, S., Higashimoto, Y., Appella, E., Minucci, S., Pandolfi, P.P., and Pelicci, P.G. (2000). PML regulates p53 acetylation and premature senescence induced by oncogenic Ras. Nature *406*, 207–210.

Pei, H., Li, L., Fridley, B.L., Jenkins, G.D., Kalari, K.R., Lingle, W., Petersen, G., Lou, Z., and Wang, L. (2009). FKBP51 affects cancer cell response to chemotherapy by negatively regulating Akt. Cancer Cell *16*, 259–266.

Pillai, R.S., Artus, C.G., and Filipowicz, W. (2004). Tethering of human Ago proteins to mRNA mimics the miRNA-mediated repression of protein synthesis. RNA *10*, 1518–1525.

Qiu, R.G., Abo, A., McCormick, F., and Symons, M. (1997). Cdc42 regulates anchorage-independent growth and is necessary for Ras transformation. Mol. Cell. Biol. *17*, 3449–3458.

Rabien, A., Sanchez-Ruderisch, H., Schulz, P., Otto, N., Wimmel, A., Wiedenmann, B., and Detjen, K.M. (2012). Tumor suppressor p16INK4a controls oncogenic K-Ras function in human pancreatic cancer cells. Cancer Sci. *103*, 169–175.

Roman, A., and Munger, K. (2013). The papillomavirus E7 proteins. Virology *445*, 138–168.

Ruas, M., and Peters, G. (1998). The p16INK4a/CDKN2A tumor suppressor and its relatives. Biochim. Biophys. Acta *1378*, F115–F177.

Samatar, A.A., and Poulikakos, P.I. (2014). Targeting RAS-ERK signalling in cancer: promises and challenges. Nat. Rev. Drug Discov. *13*, 928–942.

Scheffner, M., Werness, B.A., Huibregtse, J.M., Levine, A.J., and Howley, P.M. (1990). The E6 oncoprotein encoded by human papillomavirus types 16 and 18 promotes the degradation of p53. Cell *63*, 1129–1136.

Serrano, M., Lin, A.W., McCurrach, M.E., Beach, D., and Lowe, S.W. (1997). Oncogenic ras provokes premature cell senescence associated with accumulation of p53 and p16INK4a. Cell *88*, 593–602.

Sharma, A., Kumar, M., Aich, J., Hariharan, M., Brahmachari, S.K., Agrawal, A., and Ghosh, B. (2009). Posttranscriptional regulation of interleukin-10 expression by hsa-miR-106a. Proc. Natl. Acad. Sci. USA *106*, 5761–5766.

Shay, J.W., Pereira-Smith, O.M., and Wright, W.E. (1991). A role for both RB and p53 in the regulation of human cellular senescence. Exp. Cell Res. *196*, 33–39.

Silber, J., Lim, D.A., Petritsch, C., Persson, A.I., Maunakea, A.K., Yu, M., Vandenberg, S.R., Ginzinger, D.G., James, C.D., Costello, J.F., et al. (2008). miR-124 and miR-137 inhibit proliferation of glioblastoma multiforme cells and induce differentiation of brain tumor stem cells. BMC Med. *6*, 14.

Stephen, A.G., Esposito, D., Bagni, R.K., and McCormick, F. (2014). Dragging ras back in the ring. Cancer Cell *25*, 272–281.

Sullivan, R.J., and Flaherty, K.T. (2013). Resistance to BRAF-targeted therapy in melanoma. Eur. J. Cancer *49*, 1297–1304.

Suzuki, H.I., Yamagata, K., Sugimoto, K., Iwamoto, T., Kato, S., and Miyazono, K. (2009). Modulation of microRNA processing by p53. Nature *460*, 529–533.

Thompson, P.M., Gotoh, T., Kok, M., White, P.S., and Brodeur, G.M. (2003). CHD5, a new member of the chromodomain gene family, is preferentially expressed in the nervous system. Oncogene *22*, 1002–1011.

Tsukada, Y., Fang, J., Erdjument-Bromage, H., Warren, M.E., Borchers, C.H., Tempst, P., and Zhang, Y. (2006). Histone demethylation by a family of JmjC domain-containing proteins. Nature *439*, 811–816.

Vandesompele, J., De Preter, K., Pattyn, F., Poppe, B., Van Roy, N., De Paepe, A., and Speleman, F. (2002). Accurate normalization of real-time quantitative RT-PCR data by geometric averaging of multiple internal control genes. Genome Biol. *3*, research0034–research0034.11.

Voorhoeve, P.M., le Sage, C., Schrier, M., Gillis, A.J., Stoop, H., Nagel, R., Liu, Y.P., van Duijse, J., Drost, J., Griekspoor, A., et al. (2006). A genetic screen implicates miRNA-372 and miRNA-373 as oncogenes in testicular germ cell tumors. Cell *124*, 1169–1181.

Weber, J.D., Taylor, L.J., Roussel, M.F., Sherr, C.J., and Bar-Sagi, D. (1999). Nucleolar Arf sequesters Mdm2 and activates p53. Nat. Cell Biol. *1*, 20–26.

Welsh, C.F., Roovers, K., Villanueva, J., Liu, Y., Schwartz, M.A., and Assoian, R.K. (2001). Timing of cyclin D1 expression within G1 phase is controlled by Rho. Nat. Cell Biol. *3*, 950–957.

Whetstine, J.R., Nottke, A., Lan, F., Huarte, M., Smolikov, S., Chen, Z., Spooner, E., Li, E., Zhang, G., Colaiacovo, M., and Shi, Y. (2006). Reversal of histone lysine trimethylation by the JMJD2 family of histone demethylases. Cell *125*, 467–481.

Xiao, J., Peng, F., Yu, C., Wang, M., Li, X., Li, Z., Jiang, J., and Sun, C. (2014). microRNA-137 modulates pancreatic cancer cells tumor growth, invasion and sensitivity to chemotherapy. Int. J. Clin. Exp. Pathol. *7*, 7442–7450.

Young, A.R., Narita, M., Ferreira, M., Kirschner, K., Sadaie, M., Darot, J.F., Tavaré, S., Arakawa, S., Shimizu, S., Watt, F.M., and Narita, M. (2009). Autophagy mediates the mitotic senescence transition. Genes Dev. *23*, 798–803.

Zhang, D., Yoon, H.G., and Wong, J. (2005). JMJD2A is a novel N-CoR-interacting protein and is involved in repression of the human transcription factor achaete scute-like homologue 2 (ASCL2/Hash2). Mol. Cell. Biol. *25*, 6404–6414.

Zhang, B., Liu, T., Wu, T., Wang, Z., Rao, Z., and Gao, J. (2015). microRNA-137 functions as a tumor suppressor in human non-small cell lung cancer by targeting SLC22A18. Int. J. Biol. Macromol. *74*, 111–118.

Zhu, J., Woods, D., McMahon, M., and Bishop, J.M. (1998). Senescence of human fibroblasts induced by oncogenic Raf. Genes Dev. *12*, 2997–3007.

Zhu, X., Li, Y., Shen, H., Li, H., Long, L., Hui, L., and Xu, W. (2013). miR-137 inhibits the proliferation of lung cancer cells by targeting Cdc42 and Cdk6. FEBS Lett. *587*, 73–81.